

Artificial neural network prediction of heat-treatment hardness and abrasive wear resistance of High-Vanadium High-Speed Steel (HVHSS)

Xu Liujie · Xing Jiandong · Wei Shizhong ·
Peng Tao · Zhang Yongzhen · Long Rui

Received: 8 August 2005 / Accepted: 27 January 2006 / Published online: 2 January 2007
© Springer Science+Business Media, LLC 2006

Abstract The hardness and abrasive wear resistance were measured after High-Vanadium High-Speed Steel (HVHSS) were quenched at 900 °C–1100 °C, and then tempered at 250 °C–600 °C. Via one-hidden-layer and two-hidden-layer Back-Propagation (BP) neural networks, the non-linear relationships of hardness (H) and abrasive wear resistance (ϵ) vs. quenching temperature and tempering temperature (T_1 , T_2) were established, respectively, on the base of the experimental data. The results show that the well-trained two-hidden-layer networks have rather smaller training errors and much better generalization performance compared with well-trained one-hidden-layer neural networks, and can precisely predict hardness and abrasive wear resistance according to quenching and tempering temperatures. The prediction values have sufficiently mined the basic domain knowledge of heat treatment process of HVHSS. Therefore, a new way of predicting hardness and wear resistance according to heat treatment technique was provided by the authors.

Introduction

High speed steel with high vanadium content is one kind of newly-developed wear-resistance material that has been used for making steel rollers in some countries [1–4]. Recently, researchers have paid much attention to the applications of High-Vanadium High-Speed Steel (HVHSS) in crush industry such as hammer, jaw, rotor, etc for abrasive wear [5, 6]. The research results have shown that wear resistance of HVHSS applied for roll and crush industry is about 3–5 times higher than that of high chromium cast iron [3–7]. The excellent wear property of HVHSS depends on its microstructure, i.e., carbides and matrix. At a certain chemical composition, heat treatment technique plays a crucial role in changing matrix microstructure, such as retained austenite content and characteristics of martensite, resulting in significantly influencing on wear resistance. The previous research mainly focused on the effect of alloys and carbides on wear properties of HVHSS [1, 2, 8, 9], but neglected the effect of heat treatment conditions on wear properties. This work tested the hardnesses and wear properties after HVHSS containing 10%V was treated by different heat treatment techniques, and then predicted the effect of heat treatment temperatures on hardness and wear resistance according to the test data using artificial neural networks. So that the users can get proper heat treatment technique of HVHSS for improving wear resistance.

Neural networks are a class of flexible nonlinear models inspired by the way in which the human brain processes information. Given an appropriate number of hidden-layer units, neural networks can approximate any nonlinear function to an arbitrary degree of

X. Liujie (✉) · X. Jiandong
State Key Laboratory for Mechanical Behavior of Materials,
Xi'an Jiaotong University, Xi'an 710049, P.R. China
e-mail: wmxlj@126.com

W. Shizhong · L. Rui
Henan Engineering Research Center for Wear of Material,
Luoyang 471003, P.R. China

W. Shizhong · P. Tao · Z. Yongzhen
School of Materials Science and Engineering, Henan
University of Science and Technology, Luoyang 471003,
P.R. China

accuracy through the composition of a network of relatively simple functions [10, 11]. The flexibility and simplicity of neural networks have made them a popular modeling and forecasting tool across different research areas in recent years. A variety of different neural network models have thus developed, among which the Back-propagation (BP) network is the most widely adopted in the present study [12–14]. In this work, the non-linear relationships of the hardness (H) and abrasive wear resistance (ε) vs. quenching temperature and tempering temperature (T_1 , T_2) were established, respectively, by the use of BP networks.

Building the neural network model

Algorithm

A BP algorithm is a kind of generalized form of the least-mean-squares algorithm usually used in engineering. But the basic BP algorithm is too slow for most practical applications. In order to speed up the algorithm and make it more practical, several modifications have been proposed by researchers. The research on faster algorithm falls roughly into two categories. One involves the development of heuristic techniques such as the use of momentum and variable learning rates. The other has focused on standard numerical optimization techniques such as the conjugate gradient algorithm and the Levenberg–Marquardt algorithm. Among these algorithms, Levenberg–Marquardt algorithm is most rapid for medium networks. But it is difficult to get excellent composite of high training precision and good generalization capability in this work when Levenberg–Marquardt algorithm is employed because the data of hardness and wear resistance are very dispersive and complicate. In order to enhance the generalization capability of networks, two methods, including regularization and early stop, are often employed. Regularization constrains the size of the network parameters [15], the idea of which is that the true underlying function is assumed to have a degree of smoothness. When the parameters in a network are kept small, the network response will be smooth. Thus any modestly oversized network should be able to sufficiently represent the true function, rather than capture the noise. With regularization, the objective function becomes (1)

$$F = \gamma E_D + (1 - \gamma) E_W \quad (1)$$

where E_W is the sum of squares of the network parameters, and γ is the performance ratio, the

magnitude of which dictates the emphasis of the training. If γ is very large, then the training algorithm will drive the errors to be small. But if γ is very small, then training will emphasize parameter size reduction at the expense of network errors, thus producing a smoother network response. The optimal regularization parameter can be determined by Bayesian techniques [16]. So this work adopted Bayesian regularization in combination with Levenberg–Marquardt.

Architecture of model

Quenching temperature (T_1) and tempering temperature (T_2) play important roles in influencing hardness (H) and relative wear resistance (ε) of HVHSS when its chemical composition is certain. The target of this research is to establish non-linear relationships between the input parameters (T_1 , T_2) and the output parameters (H , ε) using BP networks. A lot of computational instances show that two hidden layers neural networks are suitable [13, 17, 18]. In this paper, compared with one-hidden-layer neural networks, two two-hidden-layer networks are built and used for predicting hardness and relative wear resistance, respectively (Fig. 1) via the neural-network toolbox of matlab6.5 [19]. For the one-hidden-layer networks, the quantity of nodes in hidden layer was determined by trial-and-error method. After trial-and-error computation for many times by the artificial neural network program developed via matlab6.5, the optimal topologies ($\{2, 7, 1\}$ and $\{2, 11, 1\}$) of two one-hidden-layer networks were gotten, respectively. For the two-hidden-layer networks, if N is the quantity of nodes in output layer and N_1 , N_2 are the quantity of nodes in the first and the second hidden layer respectively, $N_2 = N + 1$ or $N_2 = N + 2$. Adjusting N_1 ensures both the generalization performance and the rate of the convergence satisfactory. After trial-and-error computation for many times by the artificial neural network program, the perfect topologies ($\{2, 5, 3, 1\}$ and $\{2, 15, 2, 1\}$) of two two-hidden-layer neural networks were

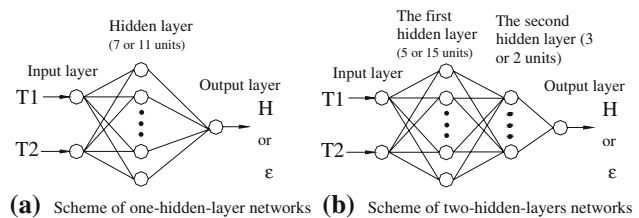


Fig. 1 Schemes of BP neural networks, **(a)** Scheme of one-hidden-layer networks, **(b)** Scheme of two-hidden-layers networks

gotten, respectively. Sigmoid and pureline transfer function was employed for hidden layers and output layer, respectively.

Training and verifying

Collecting the experimental data

The chemical composition of tested HVHSS is listed in Table 1. The knowledge of a specific field is implicated in the existing training samples, so an appropriate dataset with good distribution is significant for reliable training and performance of neural networks. To ensure reasonable distribution and enough information of the dataset, heat treatment techniques of HVHSS are covered with different quenching temperatures and tempering temperatures, as shown in Table 2. The total samples reach 30.

The alloy ingot was produced by melting the raw materials in a 50 kg intermediate frequency induction melting furnace. To improve the absorptivity of vanadium, liquid steel was deoxidized preliminarily before adding ferrovanadium, which was added in liquid steel in the final stage of melting. At the same time, the residence time of high temperature liquid steel was shortened to enable the absorptivity of vanadium to reach 90%. The final deoxidation was conducted by adding 0.1% pure aluminum. The modifying agent used was 0.4% SIII(mainly containing rare earth), which was developed by researchers. The melting alloys were tapped from the furnace at about 1500 °C, and cast at 1450 °C. The hardness of specimens was measured using an HR-150A Rockwell tester. Five points were measured for every sample, with the last value as the average of the five values. The wear test

Table 1 The chemical composition of the studied HVHSS

| Element | C | V | Cr | Mo | Si | Mn | S | P |
|-------------|------|------|------|------|------|------|------|------|
| Content/wt% | 2.98 | 9.80 | 4.25 | 2.95 | 0.65 | 0.83 | 0.05 | 0.06 |

Table 2 The heat treatment techniques of tested HVHSS

| Quenching temperature/ °C | Tempering temperature /°C | | | | | | | |
|------------------------------|---------------------------|-----|-----|-----|-----|-----|-----|-----|
| | 250 | 300 | 350 | 400 | 450 | 500 | 550 | 600 |
| 900 | + | — | + | — | + | + | + | + |
| 950 | + | + | + | — | + | + | + | + |
| 1000 | + | — | + | + | + | — | + | + |
| 1050 | + | — | + | — | + | + | + | + |
| 1100 | + | — | + | — | + | — | + | + |

+: Composite of the corresponding quenching and tempering temperatures in Table 2

was conducted on a pin-on-disk (type ML-10) friction testing machine using 120-grit alumina waterproof-abrasive sand paper. The test distance was 70 mm × 20, with pressure at 15.6 MPa. For every group, three samples were selected, and the wear loss is average result of the three repetitions. The relative wearability was specified by ϵ . $\epsilon = M_0/M$, where M_0 expresses the maximum wear loss among all the specimens, and M expresses the wear loss of each tested specimen. The wear weight losses of samples were measured using TG328B analytical balance, with range of measurement of 0–200 g and precision of 0.1 mg.

In this section, 30 experimental data of hardness and relative wear resistance were collected for building the neural network models, respectively. Among these, 25 data were selected as training data, and the others were used to verify the predicted results.

Normalization

In order to relieve the training difficulty and balance the important of each parameter during training process, the examinational data were normalized. It is recommended that the data be normalized between slightly offset values such as 0.1 and 0.9. One way to scale input and output variables in interval [0.1, 0.9] is as (2)

$$P_n = 0.1 + (0.9 - 0.1) \times (P - P_{min}) / (P_{max} - P_{min}) \tag{2}$$

Where P_n is the normalized value of P , and P_{max} and P_{min} are the maximum and minimum values of P , respectively.

After the neural network was trained, tested and simulated, it is necessary for the simulating data to be unnormalized corresponded with normalization. The unnormalized method is as (3)

$$P = (P_n - 0.1) \times (P_{max} - P_{min}) / (0.9 - 0.1) + P_{min} \tag{3}$$

Where P is the unnormalized value of P_n .

Training and verifying

Figures 2 and 3 shows the changing of sum square errors with increasing epochs for the one-hidden-layer hardness and relative wear resistance networks, respectively. The artificial neural networks achieved stable states after about 50 and 55 cycles of training, respectively, and the sum square errors of networks reach 0.0579 and 0.1239 at last, respectively (Figs. 2 and 3). The verifying

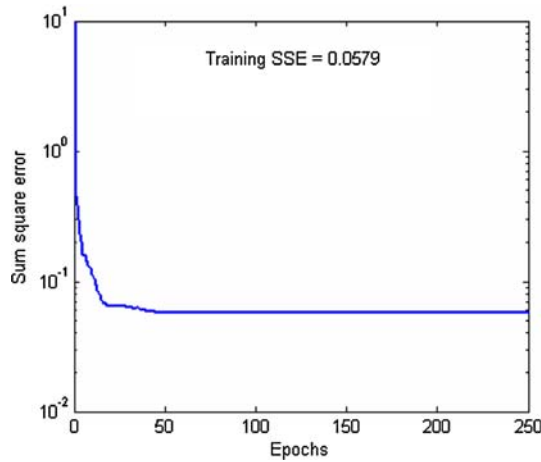


Fig. 2 The training error curve of one-hidden-layer hardness network

results of trained data are shown in Figs. 4 and 5, respectively. On the other hand, the two-hidden-layer artificial neural networks achieved stable states after about 70 and 250 cycles of training, respectively, and the sum square errors of networks reach 0.0474 and 0.0013 at last, respectively (Figs. 6 and 7). And the verifying results of trained data are shown in Figs. 8 and 9, respectively. It can be seen from Figs. 2, 3 and Figs. 6, 7 that two-hidden-layer networks have smaller training errors compared with one-hidden-layer networks. To test the generalization performance of the trained networks, the relative errors between the five test data and the corresponding predicted values from neural networks are shown in Table 3 for the one-hidden-layer networks and Table 4 for the two-hidden-layer networks, respectively. The test results in Tables 3 and 4 show that the well-trained two-hidden-layer networks

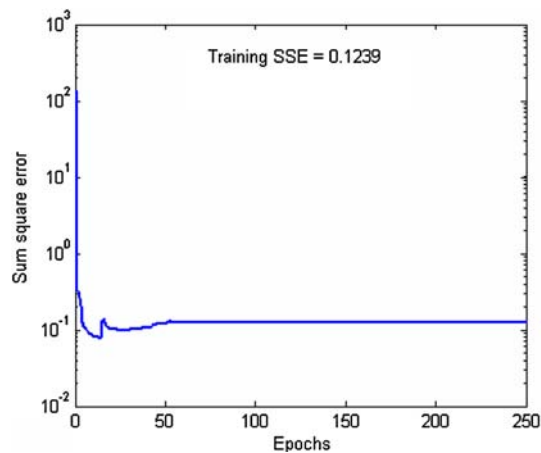


Fig. 3 The training error curve of one-hidden-layer relative wear resistance network

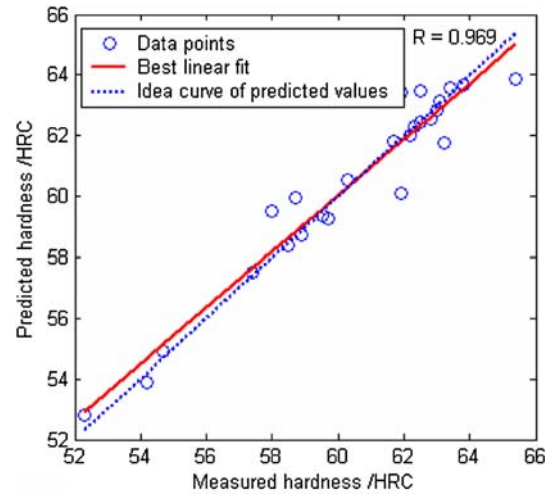


Fig. 4 Verifying results for hardness of training samples via one-hidden-layer neural network

models have much smaller test errors compared with well-trained one-hidden-layer networks models, and take on optimal generalization performance. So the well-trained two-hidden-layer networks models have greater accuracy in predicting hardness and relative wear resistance compared with one-hidden-layer networks models.

Prediction and discussion

After neural networks are trained successfully, all domain knowledge extracted out from the existing samples is stored as digital forms in weights associated with each connection between neurons. Making full use of the domain knowledge stored in the well-trained

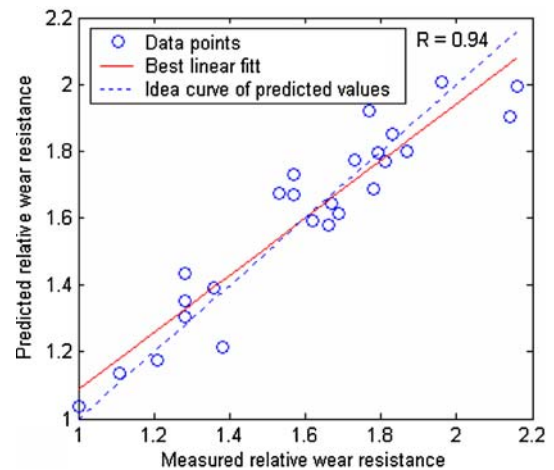


Fig. 5 Verifying results for relative wear resistance of training samples via one-hidden-layer network

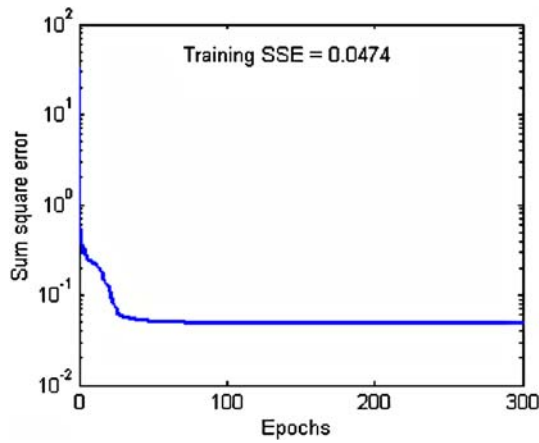


Fig. 6 The training error curve of two-hidden-layer hardness network

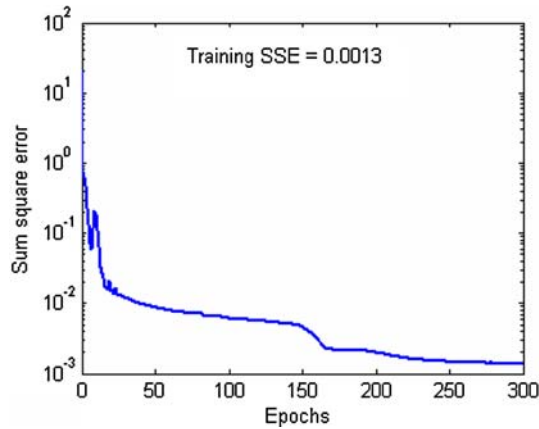


Fig. 7 The training error curve of two-hidden-layer relative wear resistance network

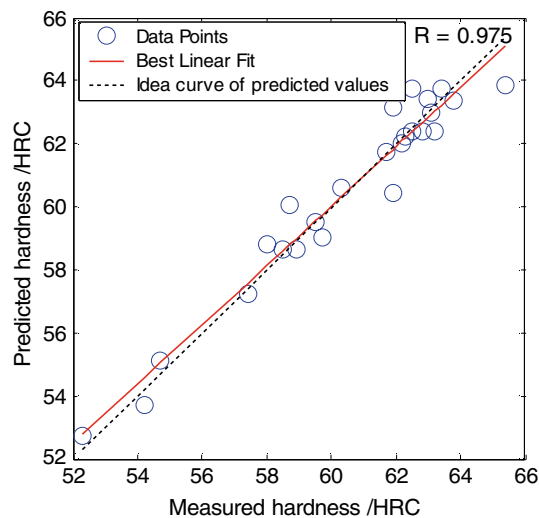


Fig. 8 Verifying results for hardness of training samples via two-hidden-layer neural network

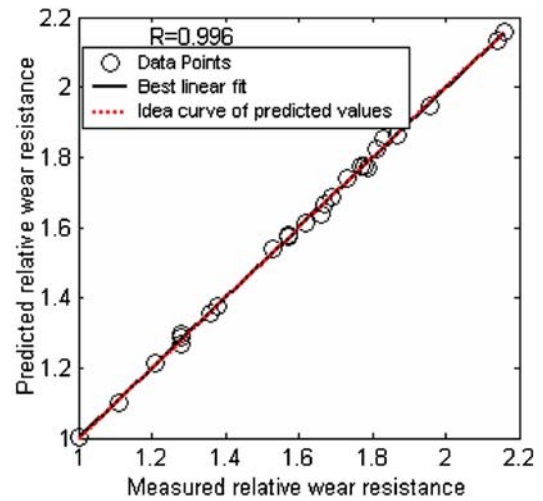


Fig. 9 Verifying results for relative wear resistance of training samples via two-hidden-layer neural network

two-hidden-layer networks, Fig. 10 through 13 were gotten, which show the relationship of hardness and relative wear resistance vs. quenching and tempering temperatures. Obviously, Fig. 10 through 13 exhibit much more professional knowledge.

The effect of heat treatment temperature on hardness

The prediction results in Figs. 10 and 11 are as follows:

- (1) At any given quenching temperature, hardness decreases slowly with tempering temperature increasing to about 450 °C–500 °C, and rises with tempering temperature continuative increasing to about 550 °C, and then decreases as tempering temperature further increases to 600 °C.
- (2) The hardness decreases with quenching temperature increasing when tempering temperature is lower than about 500 °C. When tempering temperature is higher than about 530 °C, the hardness rises as quenching temperature increases from 900 °C to 1050 °C, and then decreases rapidly as quenching temperature further increases to 1100 °C.
- (3) The peak value of hardness occurs at quenching of 1000 °C–1050 °C and tempering of 530 °C–560 °C.

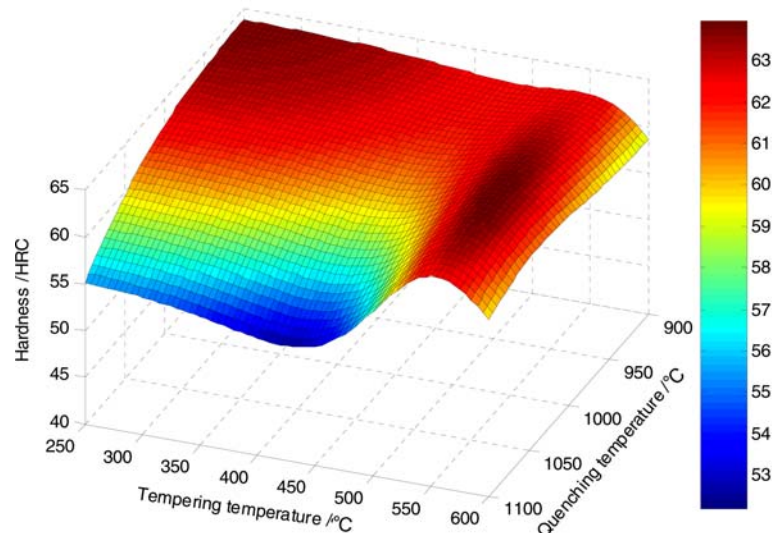
The hardness of HVHSS is mainly related to stress state and microstructure factors such as retained austenite content, characteristic of martensite, amount and type of carbides as well as tempering precipitations. In this work, heat treatment temperatures mainly influence on stress state, retained austenite content and

Table 3 The tested data, predicted values of one-hidden-layer neural networks and relative errors

| Inputs | | Hardness /HRC | | | Relative wear resistance | | |
|----------------------|----------------------|---------------|------------------|--------------------|--------------------------|------------------|---------------------|
| Quenching temp. / °C | Tempering temp. / °C | Tested data | Predicted values | Relative error / % | Tested data | Predicted values | Relative errors / % |
| 900 | 500 | 62.6 | 64.21 | 2.57 | 1.76 | 1.88 | 6.82 |
| 950 | 500 | 62.0 | 64.39 | 3.85 | 1.78 | 1.98 | 11.24 |
| 950 | 300 | 63.6 | 64.85 | 1.97 | 1.81 | 1.84 | 1.66 |
| 1000 | 400 | 60.5 | 59.57 | -1.54 | 1.59 | 1.57 | -1.26 |
| 1050 | 500 | 61.8 | 61.83 | 0.05 | 1.91 | 1.70 | -10.99 |

Table 4 The tested data, predicted values of two-hidden-layer neural networks and relative errors

| Inputs | | Hardness /HRC | | | Relative wear resistance | | |
|----------------------|----------------------|---------------|------------------|--------------------|--------------------------|------------------|---------------------|
| Quenching temp. / °C | Tempering temp. / °C | Tested data | Predicted values | Relative error / % | Tested data | Predicted values | Relative errors / % |
| 900 | 500 | 62.6 | 62.1 | -0.80 | 1.76 | 1.75 | -0.57 |
| 950 | 500 | 62.0 | 62.2 | 0.32 | 1.78 | 1.71 | -3.93 |
| 950 | 300 | 63.6 | 63.3 | -0.47 | 1.81 | 1.83 | 1.10 |
| 1000 | 400 | 60.5 | 61.1 | 0.99 | 1.59 | 1.61 | 1.26 |
| 1050 | 500 | 61.8 | 60.0 | -2.91 | 1.91 | 1.80 | -5.76 |

Fig. 10 Prediction on relationship of hardness vs. quenching and tempering temperatures using two-hidden-layer neural network

characteristic of martensite, but have not obvious effect on as-cast carbides. The decreasing of stress and decomposition of martensite will lead to decreasing hardness. But the transformation of retained austenite to martensite during tempering will cause the increasing of hardness. Besides, fine carbide precipitations during tempering will cause secondary hardening of HVHSS, resulting in increasing overall hardness also. So the changing of hardness depends on the composite of four factors above.

At any given quenching temperature, with increasing tempering temperature from 250 °C to 450 °C–500 °C, the retained stress of quench decreases rapidly, but the

retained austenite content in matrix decreases slowly [20], resulting in the slightly decreasing of hardness. While with further increasing tempering temperature to 550 °C, the retained austenite content rapidly decreases because of the transformation of retained austenite to martensite [20], therefore plays a main role in determining hardness, resulting in the increasing of hardness. However, with tempering temperature increasing from 550 °C to 600 °C, the hardness decreases because of decomposition of some martensite.

In the process of quenching of HVHSS, the higher the austenitizing temperature is, the more the carbon and alloys, including Cr, Mo and V, dissolving in

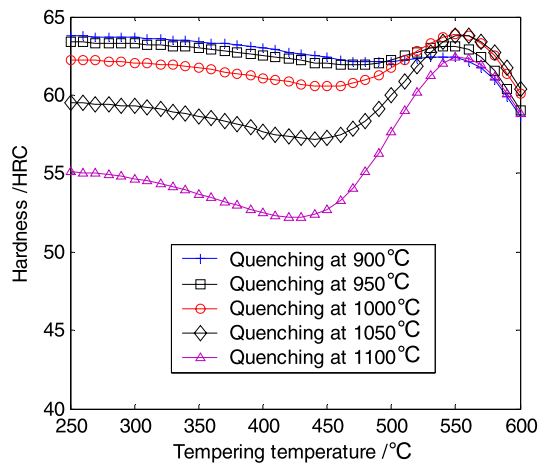
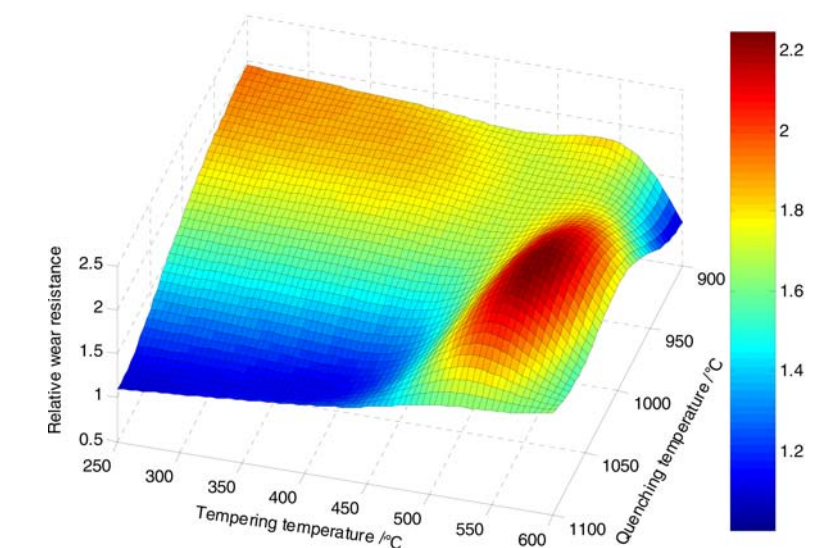


Fig. 11 Prediction on the effect of temper temperature on hardness using two-hidden-layer neural network

austenite are. This will lead to the increasing of austenite stability because Cr, Mo and V elements can stabilize austenite. As a result, retained austenite content will rise with increasing quenching temperature at any given tempering temperatures. At tempering temperature of lower than about 450 °C–500 °C, there are slight retained austenite transformed to martensite. Therefore, the retained austenite content plays a main role in determining hardness, resulting in gradually decreasing hardness with increasing quenching temperature. When the tempering temperature is higher than about 530 °C, the secondary hardening occurs because of fine carbide precipitations from matrix. If the quenching temperature is very low, very small amount of alloys dissolving in matrix will cause small amounts of carbide precipitations and poor secondary hardening capability during high-tempera-

Fig. 12 Prediction on the relationship of relative wear resistance vs. quenching and tempering temperatures using two-hidden-layer network



ture temper. With increasing quenching temperature, the increasing of alloys dissolving in matrix will lead to the enhanced secondary hardening capability, therefore increasing overall hardness of HVHSS. However, exorbitant quenching temperature will cause superabundant retained austenite in matrix, reduced difficulty even during high tempering temperature, and plays a crucial role in determining hardness, therefore decreasing overall hardness of HVHSS.

At quenching temperature of 1000 °C–1050 °C and tempering temperature of 530 °C–560 °C, the tested HVHSS possesses optimal secondary hardening capability and proper retained austenite content, and therefore possesses maximum values of hardness.

The effect of heat treatment temperature on relative wear resistance

Figs. 12 and 13 show the relationship of relative wear resistance vs. quenching and tempering temperatures. As can be seen from Figs. 12 and 13,

- (1) At quenching temperature of 900 °C–1050 °C, the relative wear resistance nearly takes on the same changing tendency as hardness with tempering temperature increasing from 250 °C to 600 °C. But the relative wear resistance increases nearly linearly with increasing tempering temperature at quenching temperature of 1100 °C.
- (2) Relative wear resistance decreases with increasing quenching temperature at low tempering temperature. When tempering temperature is higher than about 530 °C, it increases to maximum as quenching temperature increases to

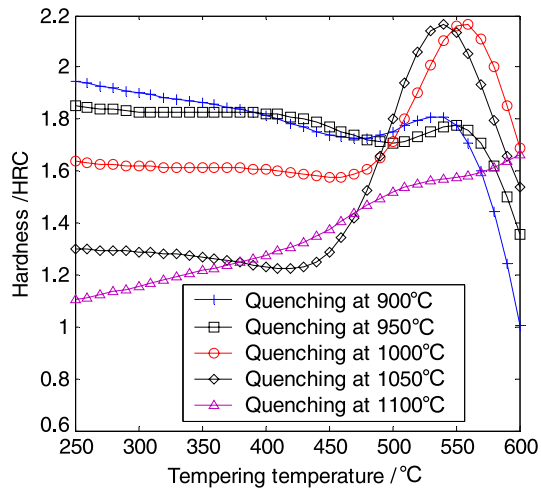


Fig. 13 Prediction on the effect of temper temperature on relative wear resistance using two-hidden-layer neural network

1000 °C–1050 °C, and then decreases as quenching temperature further increases to 1100 °C.

- (3) The optimal relative wear resistance is acquired when HVHSS is quenched at 1000 °C–1050 °C and then tempered at 530 °C–560 °C, corresponding to the peak value of hardness.

The wear resistance of HSS is closely related to microstructures and mechanical properties. In this work, the wear resistance of HVHSS mainly depends on retained austenite content and hardness. In general, the transformation of retained austenite to martensite will cause the increasing of hardness, resulting in the increasing of wear resistance. However, much lower retained austenite content also does harm to wear resistance because of the decreasing resistance to crack initiation and propagation during abrasive wear [21]. The HVHSS with higher hardness possesses stronger capacity to resist scratch of Al_2O_3 -abrasive, and therefore possesses more excellent wear resistance. As a result, at quenching temperature of 900 °C–1050 °C, the higher hardness after temper is, the more excellent relative wear resistance of HVHSS has. Besides, the ultimate decreasing of wear resistance at high tempering is also related to very small amount of retained austenite, which can resist the crack initiation and propagation during abrasive wear. But at quenching of 1100 °C, there are too much retained austenite in matrix, which plays a crucial role in determining wear resistance compared with other factors. With increasing tempering temperature, the retained austenite content rapidly decreases, accordingly, continuously increasing wear resistance.

At low tempering temperature, the relative wear resistance of HVHSS gradually decreases with

increasing quenching temperature because of the increasing retained austenite content. When tempering temperature is higher than about 530 °C, as the quenching temperature ranging from 900 °C–950 °C to 1000 °C–1550 °C, the secondary hardening capability of HVHSS gets optimal gradually and the proper retained austenite content in matrix was acquired, resulting in increasing wear resistance. But the further enhancing of quenching temperature will lead to the increasing of much retained austenite in matrix even after HVHSS was tempered at higher tempering temperature, resulting in the decreasing of wear resistance.

At quenching and tempering temperatures of 1000 °C–1050 °C and 530 °C–560 °C respectively, the composites of optimal secondary hardening capability, proper retained austenite content and maximum values of hardness result in the most excellent wear resistance of HVHSS.

Conclusions

- (1) The none-linear relationship of hardness (H) and relative wear resistance (ε) vs. quenching temperature and tempering temperature (T1, T2) could be built by BP artificial neural networks. The results show that the well-trained two-hidden-layer networks have rather smaller training errors and much better generalization performance compared with well-trained one-hidden-layer neural networks, and can precisely predict hardness and abrasive wear resistance according to quenching and tempering temperatures.
- (2) The prediction results show that the optimal relative wear resistance is acquired after HVHSS is quenched at 1000 °C–1050 °C and then tempered at 530 °C–560 °C, corresponding to the peak value of hardness. So the optimal heat treatment technique of HVHSS has been acquired.
- (3) The prediction results have sufficiently mined the basic domain knowledge of relationship of hardness and relative wear resistance vs. heat treatment techniques of HVHSS. Therefore, a new way of predicting hardness and relative wear resistance according to heat treatment technique has been provided by the authors.

Acknowledgements This work is supported by Key Scientific and Technological Breakthrough Project of Henan Province, China (No.0322020300).

References

1. Kim CK, Park JI, Lee S, Kim YC, Kim NJ, Yang JS (2005) *Metall Mater Trans* 36A:87
2. Kim SW, Lee UJ, Woo KD, Kim DK (2003) *Mater Sci Technol* 19:1727
3. Hwang KC, Lee S, Lee DHC (1998) *Mater Sci Eng A254*:282
4. Li CS, Liu XH, Wang GD, Yang G (2002) *Mater Sci Technol* 18:1581
5. Wei S, Zhu J, Xu L (2005) *Trans Mater Heat Treat* 26:44
6. Wei SZ, Long R (2001) *Cement* 8:31
7. Sano Y, Hattori T, Haga M (1992) *ISIJ Int* 32:1194
8. Park JW, Lee HC, Lee S (1999) *Metall Mater Trans* 30:399
9. Liu H, Liu Y, Yu S (2000) *Tribol* 20(6):401
10. White H (1990) *Neural Netw* 3:535
11. Altinkok N, Koker R (2005) *J Mater Sci* 40:1767
12. Reddy NS, Prasada Rao AK, Chakraborty M, Murty BS (2005) *Mater Sci Eng A391*:131
13. Su J, Dong Q, Liu P, Li H, Kang B (2003) *J Wuhan Univ Technol-Mat Sci Edit* 18:50
14. Sahoo GB, Ray C, Wade HF (2005) *Ecol Model* 183:29–46
15. Mackay, David JC (1992) *Neural Comput* 4:415
16. Gençay R, Min Q (2001) *IEEE Trans Neural Netw* 12:726
17. Liu P, Lei J, Jing X, Tian B (2005) *Trans Mater Heat Treat* 26:86
18. Su J, Dong Q, Liu P, Li H, Kang B (2003) *Trans Nonferrous Met Soc China* 13:1419
19. Guo J, Yang Z, in “Analysis and Design of Neural Network Based on Matlab6.5”(Publishing House of Electronics Industry, Beijing, 2003) pp 313
20. Wei S, Zhu J, Long R (2004) *Hot Work Technol* 12:31
21. Tong J, Zhang W (1994) *Chinese J Mech Eng* 30:103